ESI to accompany:

Sticking and patching: tuning and anchoring cyclometallated ruthenium(II) complexes

Cathrin D. Ertl, Daniel P. Ris, Stefan C. Meier, Edwin C. Constable, Catherine E. Housecroft, Markus Neuburger and Jennifer A. Zampese

Infrared spectroscopic data for the $[Ru(bpy)_2(C^N)][PF_6]$ complexes and $[Ru(bpy)_2(\mathbf{8})]$:

$[Ru(bpy)_2(\mathbf{1})][PF_6]$
IR (solid, ν/cm^{-1}): 3074 (w), 3030 (w), 1984 (w), 1911 (w), 1740 (w), 1602 (w), 1585 (m), 1563 (w), 1549 (m), 1472 (m), 1460 (m), 1443 (m), 1405 (w), 1376 (w), 1310 (w), 1297 (w), 1260 (m), 1232 (m), 1218 (w), 1179 (w), 1164 (m), 1157 (m), 1120 (w), 1108 (w), 1067 (w), 1059 (w), 1043 (w), 1028 (w), 1015 (w), 1005 (w), 957 (w), 937 (w), 884 (m), 831 (s), 813 (s), 759 (s), 727 (s), 661 (m), 651 (m), 639 (w), 598 (w), 555 (s), 472 (w).

$[Ru(bpy)_2(\mathbf{2})][PF_6]$
IR (solid, ν/cm^{-1}): 2971 (w), 2922 (w), 1964 (w), 1740 (w), 1598 (m), 1582 (m), 1557 (m), 1459 (m), 1442 (m), 1420 (m), 1377 (m), 1315 (w), 1300 (w), 1263 (m), 1232 (m), 1217 (m), 1158 (m), 1122 (w), 1104 (w), 1058 (w), 1031 (w), 1014 (m), 1004 (m), 954 (w), 885 (m), 828 (s), 773 (m), 755 (s), 742 (s), 725 (s), 674 (m), 663 (m), 653 (m), 647 (m), 572 (w), 555 (s), 525 (m), 489 (w), 467 (w).

$[Ru(bpy)_2(\mathbf{3})][PF_6]$
IR (solid, ν/cm^{-1}): 3071 (w), 2923 (w), 2852 (w), 1980 (w), 1725 (w), 1599 (w), 1577 (m), 1545 (m), 1459 (m), 1442 (m), 1421 (m), 1387 (w), 1308 (m), 1272 (m), 1258 (m), 1240 (m), 1210 (m), 1159 (m), 1123 (w), 1057 (w), 1038 (m), 1026 (m), 1015 (m), 999 (m), 878 (w), 830 (s), 756 (s), 728 (s), 662 (m), 652 (m), 610 (w), 584 (m), 555 (s), 470 (m).

$[Ru(bpy)_2(\mathbf{4})][PF_6]$
IR (solid, ν/cm^{-1}): 3074 (w), 2921 (w), 2851 (w), 1979 (w), 1706 (m), 1632 (w), 1599 (w), 1575 (w), 1559 (w), 1462 (m), 1443 (m), 1422 (m), 1375 (w), 1298 (w), 1268 (s), 1243 (m), 1220 (m), 1191 (w), 1159 (w), 1110 (m), 1056 (w), 1031 (w), 1016 (w), 1004 (w), 970 (w), 878 (w), 831 (s), 755 (s), 728 (s), 688 (m), 665 (w), 654 (m), 556 (s), 487 (w), 470 (w).

$[Ru(bpy)_2(\mathbf{5})][PF_6]$
IR (solid, ν/cm^{-1}): 3073 (w), 2960 (w), 2921 (w), 2859 (w), 1733 (w), 1598 (w), 1555 (w), 1461 (s), 1443 (m), 1416 (m), 1362 (w), 1309 (w), 1294 (w), 1257 (w), 1160 (w), 1092 (w), 1054 (w), 1029 (w), 1015 (w), 1002 (w), 878 (w), 832 (s), 756 (s), 728 (s), 700 (w), 653 (w), 602 (w), 556 (s), 530 (w), 470 (w).

$[Ru(bpy)_2(\mathbf{6})][PF_6]$
IR (solid, ν/cm^{-1}): 3072 (w), 2970 (w), 2923 (w), 2851 (w), 1958 (w), 1740 (w), 1599 (w), 1560 (w), 1464 (m), 1444 (m), 1422 (m), 1367 (m), 1312 (w), 1292 (m), 1262 (m), 1228 (w), 1218 (w), 1145 (s), 1103 (m), 1088 (m), 1067 (m), 1053 (m), 1028 (m), 1005 (w), 969 (w), 950 (m), 890 (w), 884 (w), 831 (s), 800 (s), 782 (s), 758 (s), 750 (s), 743 (s), 730 (s), 696 (m), 665 (w), 655 (m), 648 (m), 593 (w), 555 (s), 548 (s), 530 (m), 489 (m), 473 (w).

$[Ru(bpy)_2(\mathbf{7})][PF_6]$
IR (solid, ν/cm^{-1}): 2955 (w), 2922 (w), 2851 (w), 1962 (w), 1722 (m), 1600 (w), 1574 (w), 1550 (w), 1537 (w), 1460 (m), 1452 (m), 1443 (m), 1422 (m), 1404 (m), 1377 (w), 1318 (m), 1309 (m), 1270 (m), 1252 (m), 1239 (m), 1158 (w), 1118 (m), 1054 (w), 1037 (w), 1012 (m), 969 (w), 877 (w), 831 (s), 758 (s), 728 (s), 654 (m), 634 (w), 556 (s), 468 (w).

$[Ru(bpy)_2(\mathbf{8})]$
IR (solid, ν/cm^{-1}): 3317 (w), 2957 (w), 2922 (w), 2853 (w), 1596 (w), 1574 (w), 1548 (w), 1531 (w), 1458 (m), 1418 (w), 1400 (w), 1362 (m), 1285 (w), 1260 (w), 1241 (w), 1155 (w), 1120 (w), 1095 (w), 1054 (w), 1013 (w), 875 (w), 839 (s), 763 (s), 737 (s), 730 (s), 695 (w), 652 (m), 635 (w), 557 (m), 470 (w).

$[Ru(bpy)_2(\mathbf{9})][PF_6]$
IR (solid, ν/cm^{-1}): 2975 (w), 1740 (w), 1602 (w), 1575 (w), 1525 (w), 1461 (m), 1443 (w), 1421 (w), 1383 (w), 1367 (w), 1309 (w), 1298 (w), 1235 (m), 1159 (w), 1133 (w), 1098 (w), 1048 (m), 1015 (m), 965 (w), 877 (w), 832 (s), 759 (s), 729 (m), 686 (w), 655 (w), 636 (w), 576 (m), 555 (s), 518 (w).

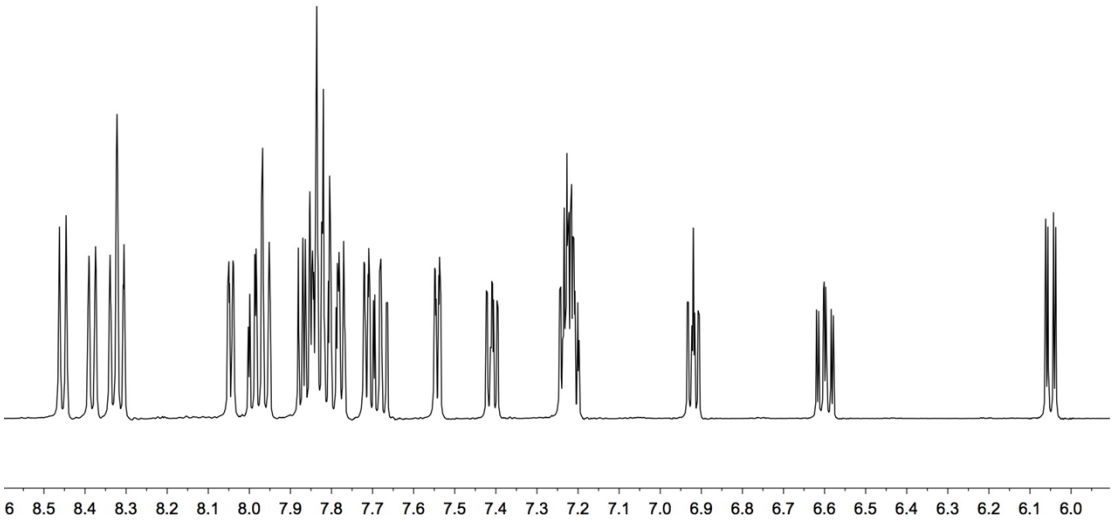

Fig. S1 500 MHz ^{1}H NMR spectrum of [Ru(bpy)$_2$(**1**)][PF$_6$] in CD_3CN

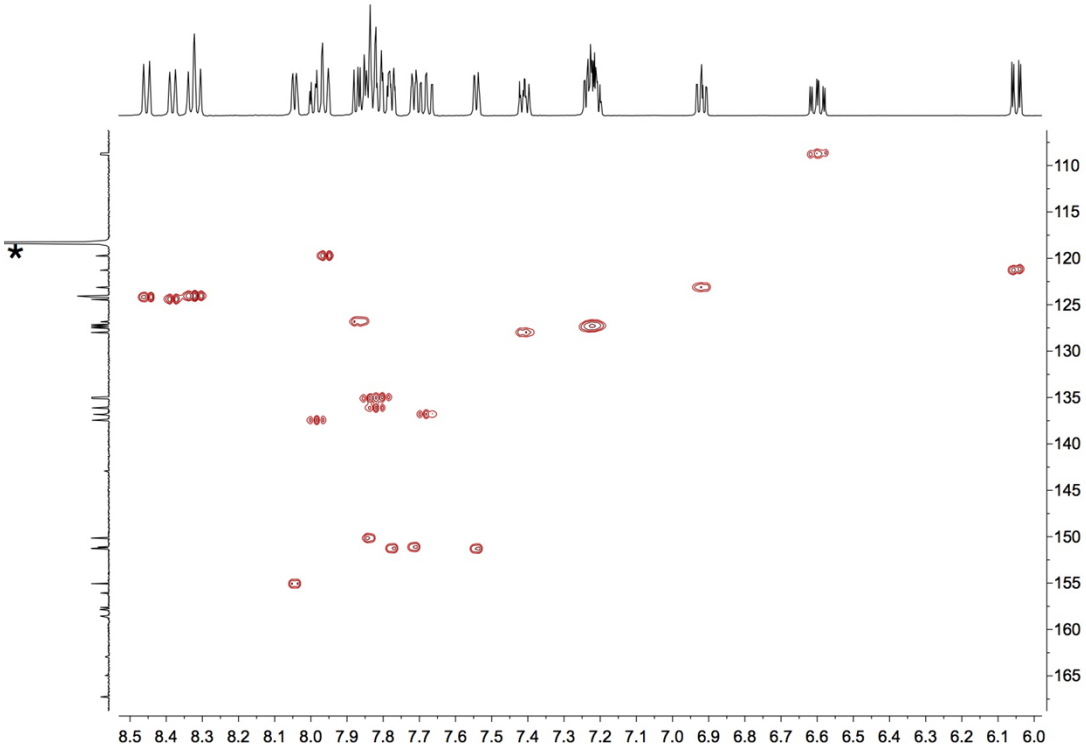

Fig. S2 500 MHz HMQC spectrum of [Ru(bpy)$_2$(**1**)][PF$_6$] in CD_3CN; (the peak in the ^{13}C NMR trace labelled * arises from CD_2CN)

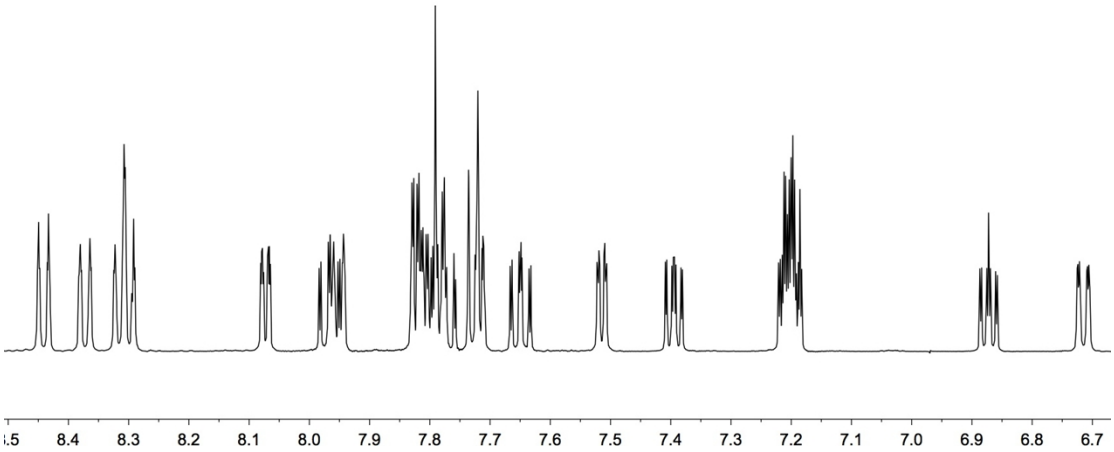

Fig. S3 Aromatic region of the 500 MHz ^{1}H NMR spectrum of [Ru(bpy)$_2$(**2**)][PF$_6$] in CD_3CN.

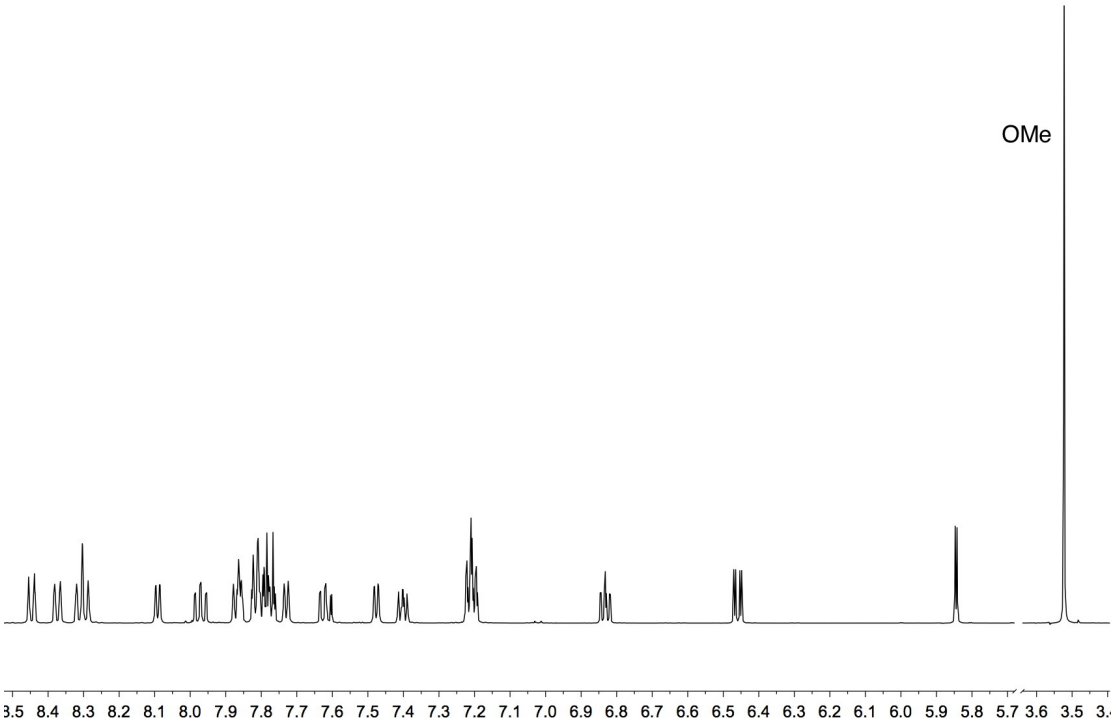

Fig. S4 500 MHz ^{1}H NMR spectrum of [Ru(bpy)$_2$(**3**)][PF$_6$] in CD_3CN.

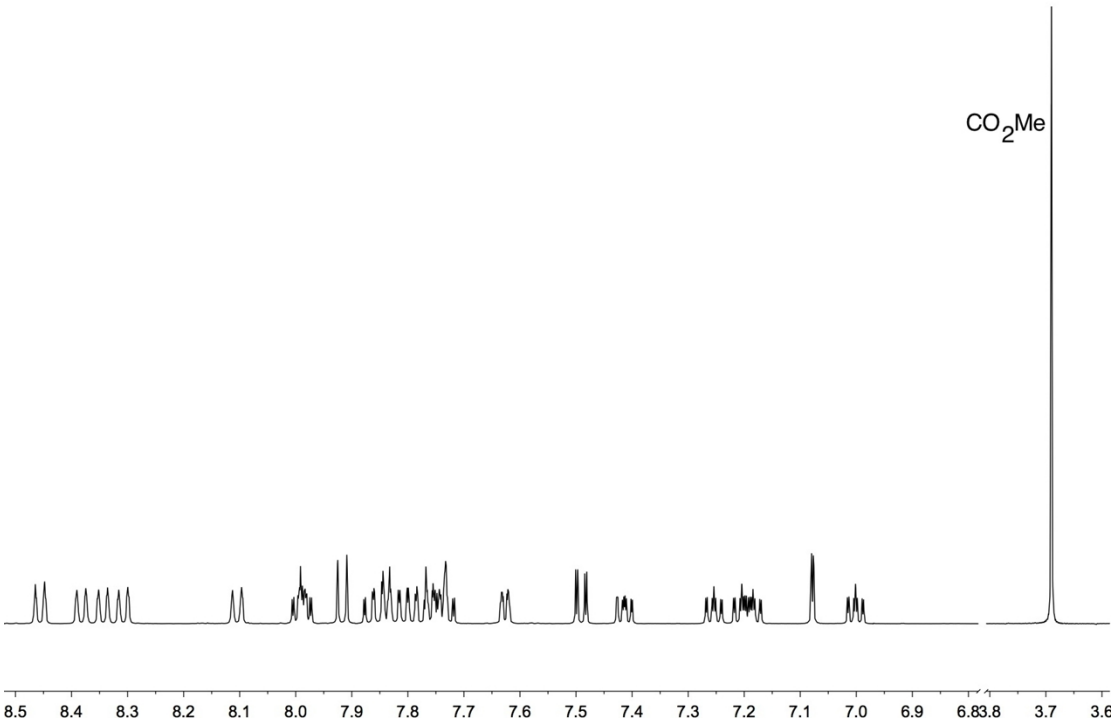

Fig. S5 500 MHz ^{1}H NMR spectrum of [Ru(bpy)$_2$(**4**)][PF$_6$] in CD$_3$CN.

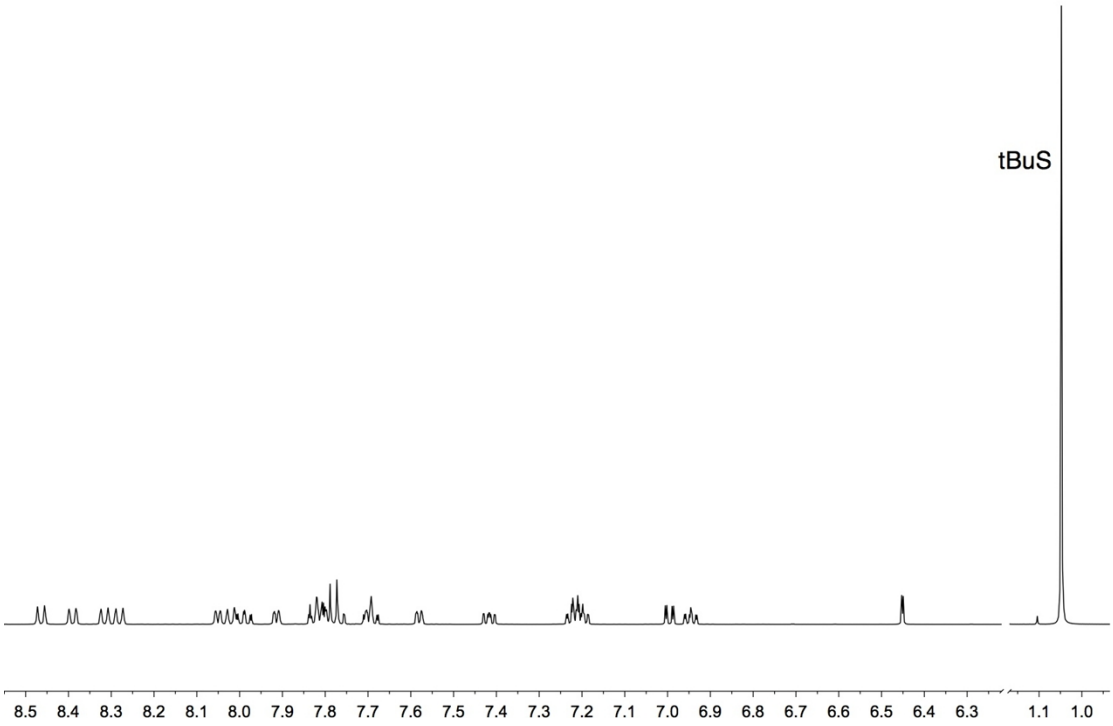

Fig. S6 500 MHz ^{1}H NMR spectrum of [Ru(bpy)$_2$(**5**)][PF$_6$] in CD$_3$CN.

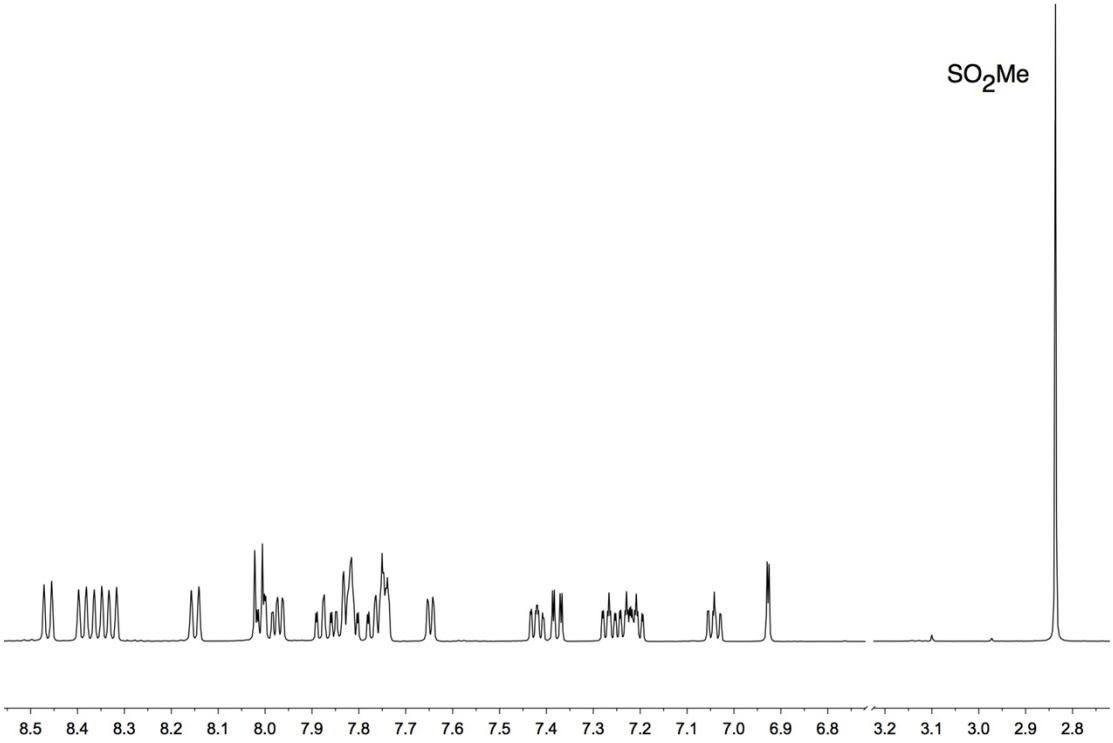

Fig. S7 500 MHz ^{1}H NMR spectrum of [Ru(bpy)$_2$(**6**)][PF$_6$] in CD$_3$CN.

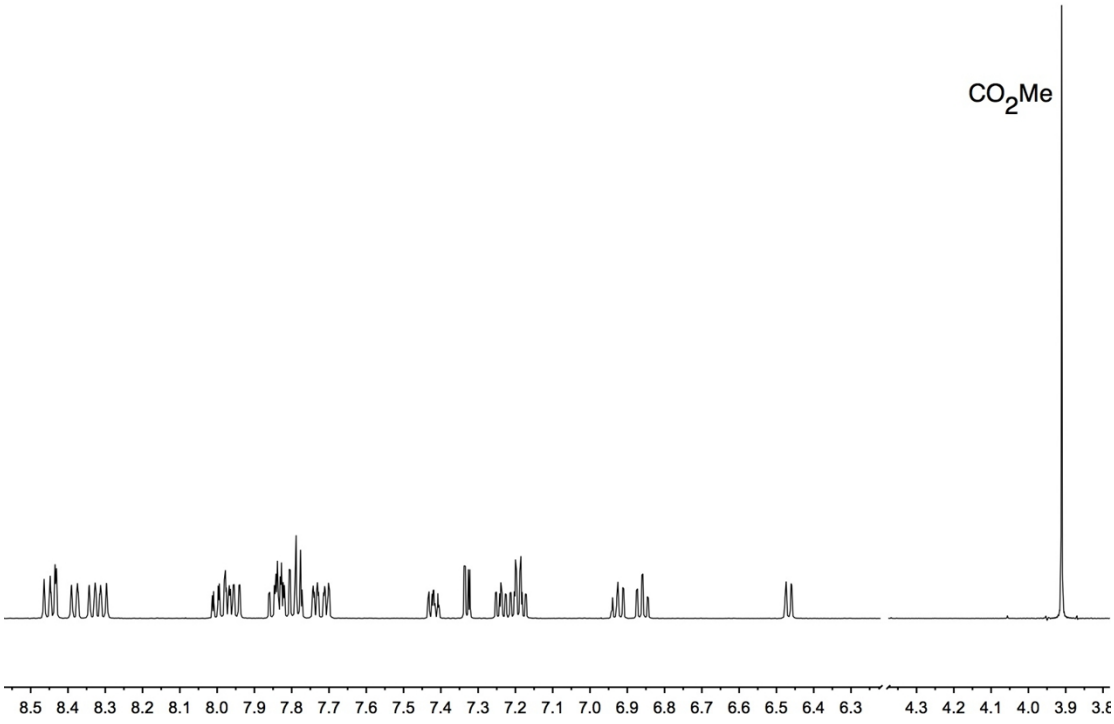

Fig. S8 500 MHz ^{1}H NMR spectrum of [Ru(bpy)$_2$(**7**)][PF$_6$] in CD$_3$CN.

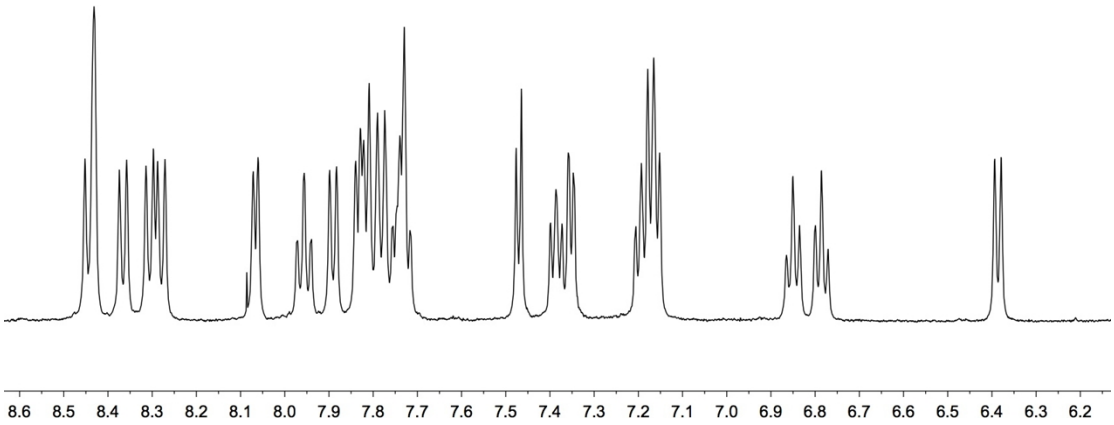

Fig. S9 500 MHz ^{1}H NMR spectrum of the neutral complex [Ru(bpy)$_2$(**8**)] in CD_3CN.

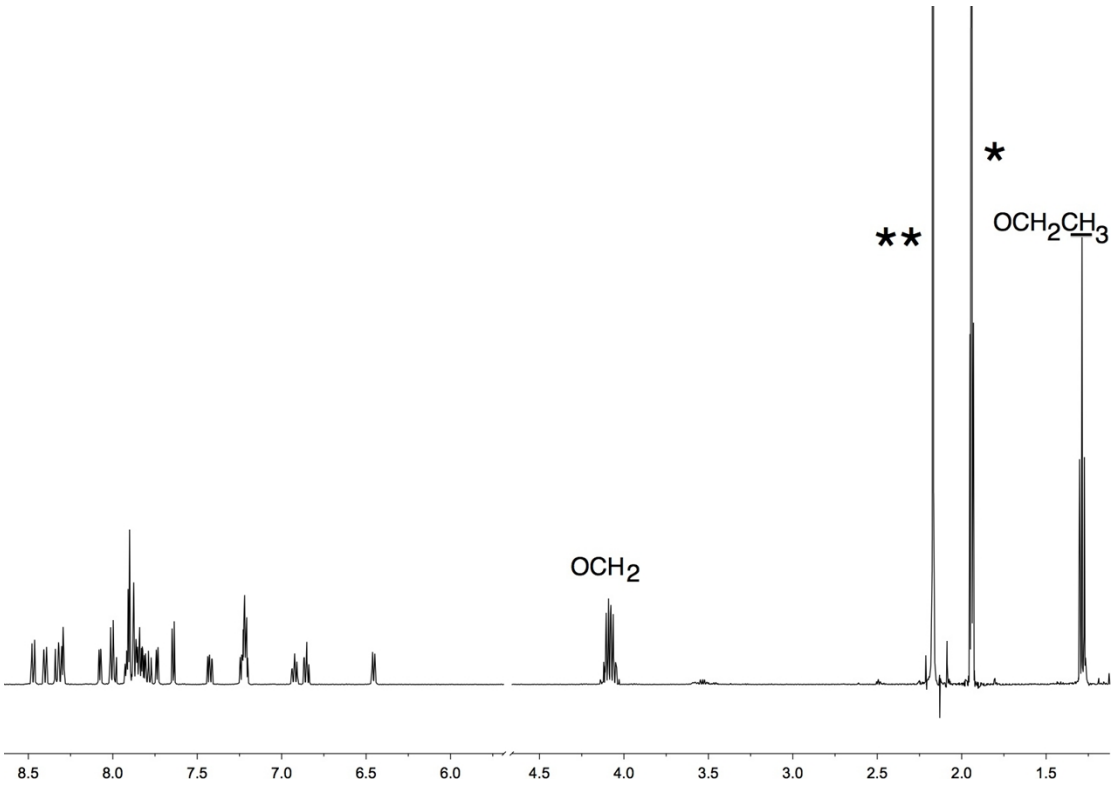

Fig. S10 500 MHz ^{1}H NMR spectrum of [Ru(bpy)$_2$(**9**)][PF_6] in CD_3CN. * = residual CD_2HCN; ** = H_2O